ARMY RESEARCH LABORATORY

Modal Decomposition Matrix (MDM) Method for Directly Calculating the Far Field of an Open Rectangular Waveguide with an Infinite Flange

by Gregory Mitchell and Dr. Wasyl Wasylkiwskyj

ARL-TR-6536 **July 2013**

NOTICES

Disclaimers

Army Research Laboratory
Adelphi, MD 20783-1197

ARL-TR-6536 **July 2013**

Modal Decomposition Matrix (MDM) Method for Directly Calculating the Far Field of an Open Rectangular Waveguide with an Infinite Flange

Gregory Mitchell and Dr. Wasyl Wasylkiwskyj
Sensors and Electron Devices Directorate, ARL

REPORT DOCUMENTATION PAGE			*Form Approved* *OMB No. 0704-0188*

1. REPORT DATE *(DD-MM-YYYY)*	**2. REPORT TYPE**	**3. DATES COVERED (From - To)**
July 2013	Final	January 1, 2011 to April 1, 2013

4. TITLE AND SUBTITLE	**5a. CONTRACT NUMBER**
Modal Decomposition Matrix (MDM) Method for Directly Calculating the Far Field of an Open Rectangular Waveguide with an Infinite Flange	
	5b. GRANT NUMBER
	5c. PROGRAM ELEMENT NUMBER
6. AUTHOR(S)	**5d. PROJECT NUMBER**
Gregory Mitchell and Dr. Wasyl Wasylkiwskyj	6362.1
	5e. TASK NUMBER
	5f. WORK UNIT NUMBER
7. PERFORMING ORGANIZATION NAME(S) AND ADDRESS(ES)	**8. PERFORMING ORGANIZATION REPORT NUMBER**
U.S. Army Research Laboratory ATTN: RDRL-SER-M 2800 Powder Mill Road Adelphi, MD 20783-1197	ARL-TR-6536
9. SPONSORING/MONITORING AGENCY NAME(S) AND ADDRESS(ES)	**10. SPONSOR/MONITOR'S ACRONYM(S)**
	11. SPONSOR/MONITOR'S REPORT NUMBER(S)

12. DISTRIBUTION/AVAILABILITY STATEMENT

Approved for public release; distribution unlimited.

13. SUPPLEMENTARY NOTES

14. ABSTRACT

The radiation from a rectangular waveguide with a perfectly conducting infinite flange is determined using the modal decomposition matrix (MDM) method. This method uses the tangential boundary condition at the aperture to directly compute the far-field radiation patterns. The fields in the waveguide are expanded in terms of waveguide modes consistent with the approach of Felsen and Marcuvitz. The radiated field is expanded as an inverse Fourier transform and represented at the aperture in terms of the discretization of the free-space transverse wave number. The results of the MDM approach are compared to numerical models using commercial software.

15. SUBJECT TERMS

Semi-infinite rectangular waveguide, infinite flange, aperture fields

16. SECURITY CLASSIFICATION OF:			**17. LIMITATION OF ABSTRACT**	**18. NUMBER OF PAGES**	**19a. NAME OF RESPONSIBLE PERSON**
					Gregory Mitchell
a. REPORT	**b. ABSTRACT**	**c. THIS PAGE**			**19b. TELEPHONE NUMBER** (*Include area code*)
Unclassified	Unclassified	Unclassified	UU	32	(301) 394-2322

Standard Form 298 (Rev. 8/98)
Prescribed by ANSI Std. Z39.18

Contents

List of Figures **iv**

1. Introduction **1**

2. Modal Decomposition of a Rectangular Waveguide **1**

2.1 Incident TE_{10} Mode Case 2

3. Formulation of the MDM Method **6**

3.1 Derivation of MDM Equation....... 6

3.2 Representation of k_x and k_y when $z \geq 0^+$ 8

4. Calculation of Far Field and Comparison to Simulation **10**

4.1 Description of CST Model 10

4.2 Results and Analysis 12

5. Conclusions **14**

6. References **15**

Appendix. Derivation of Surface Integrals for Rectangular Aperture **17**

List of Symbols, Abbreviations, and Acronyms **24**

Distribution List **25**

List of Figures

Figure 1. (a) Illustration of the boundary between the waveguide and free space at z=0. The thickness of the radiating aperture is assumed to be negligible in comparison to the wavelength. (b) Illustration of a transverse cross section of the waveguide. Again the thickness of the ground plane around the waveguide is assumed to be negligible in comparison to wavelength, i.e., less than the skin depth. 2

Figure 2. Plot of the values of k_x and k_y obtained for $\phi = 0$. 9

Figure 3. Plot of the values of k_x and k_y obtained for $\phi = \pi/4$. 10

Figure 4. (a) Transverse plane of the waveguide port. The waveguide has dimensions |a| x |b| and is surrounded by an infinite conducting flange. (b) This shows the z-direction of the waveguide with the waveguide port included. 11

Figure 5. Illustration of the mode distribution in the rectangular waveguide of the infinite flange simulation in units of V/m. 12

Figure 6. (a) Polar plot (b) Linear plot - of the far field E_θ and E_ϕ normalized radiation patterns. 13

Figure 7. Plot of the singular values of the MDM in descending order. 14

1. Introduction

The analysis of the radiating infinite flange problem has been widely studied and different methods for determining the aperture fields are presented in the published literature (*1–3*). In practice, flush mounted aperture antennas are widely used and are often approximated by an aperture in an infinite conducting surface (infinite flange). Furthermore, the solutions determined by these methods reasonably approximate those of a radiating waveguide with no infinite conducting surface (*4*). Although accurate, these methods require the rigorous calculation of the fields at the aperture of the waveguide.

This report illustrates a more straightforward approach that directly computes the radiated far field eliminating the direct calculation of the aperture field. This approach uses a modal decomposition matrix (MDM) method based on the sampling of the transverse free space wave number to determine the spectral coefficients of the widely used stationary phase approach. The results determined by our method are compared to the far-field radiation patterns achieved using CST Studio Suite software for the same problem.

2. Modal Decomposition of a Rectangular Waveguide

This section describes the theory of matching the transverse electric and magnetic fields that exist inside a uniform rectangular waveguide to those of the radiated far fields in free space. The modal decomposition described here is based on the theory published by Felsen and Marcuvitz (*5, 9*). The transverse field inside the guide is assumed to be generated from the dominant propagating mode inside the waveguide. The dominant mode is determined by the lowest cutoff frequency in the waveguide and for a rectangular waveguide the transverse electric (TE_{10}) mode is the dominant mode.

By matching tangential boundary conditions at the aperture, a system of equations is derived that will directly yield the Fourier transform of the transverse aperture field. Based on this, we can use the stationary phase approximation to calculate the far-field radiation patterns.

Figure 1 shows two orientations of the same rectangular waveguide. A half-space boundary exists at the aperture (z = 0), as depicted in figure 1a, and the waveguide extends to $-\infty$ in the negative z-direction. This is known as the semi-infinite waveguide approximation (*5*). Using this approximation, we can construct the form of the electric and magnetic fields that exist inside the waveguide due to an incident TE_{10} mode.

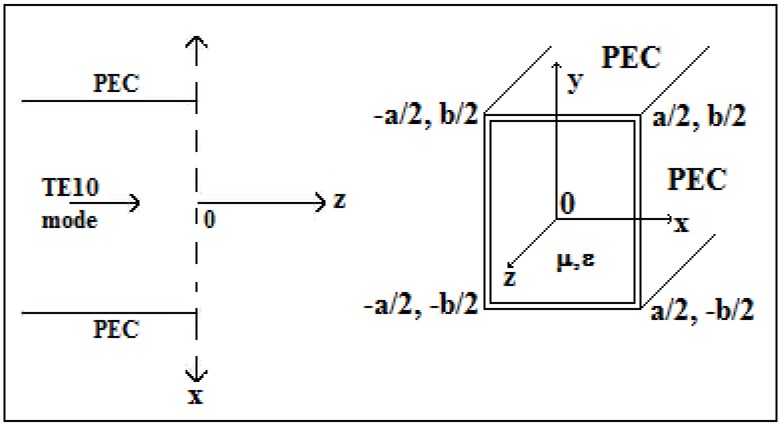

Figure 1. (a) Illustration of the boundary between the waveguide and free space at $z = 0$. The thickness of the PEC walls is assumed to be negligible in comparison to the wavelength. (b) Illustration of a transverse cross section of the waveguide. Again the thickness of the ground plane around the waveguide is assumed to be negligible in comparison to wavelength, i.e., less than the skin depth.

2.1 Incident TE_{10} Mode Case

The incident TE_{10} mode shown in figure 1a is assumed to exist inside the waveguide with the following form:

$$\underline{E}_{Tinc}\left(\underline{r}\right) = \underline{e}''_N(x,y)V\left(z\right) \tag{1a}$$

$$\underline{H}_{Tinc}\left(\underline{r}\right) = \underline{h}''_N(x,y)I\left(z\right) \tag{1b}$$

where $V(z)$ and $I(z)$ are the voltage and current at point z inside the waveguide, and are defined by solutions to the wave equation. The subscript N denotes that this is the incident mode impingent on the aperture ($z = 0$) and the superscript ’’ denotes that this is a TE mode. The superscript ’ is used to denote the transverse magnetic (TM) mode. The mode functions $\underline{e}_\upsilon(x,y)$ and $\underline{h}_\upsilon(x,y)$ are defined as

$$\begin{aligned}\underline{e}'_\upsilon(x,y) &= -\nabla_T \Phi_\upsilon(x,y) \\ &= -A'_\upsilon\left[\underline{x}_o \frac{m\pi}{a}\cos\left(\frac{m\pi}{a}\left(x+\frac{a}{2}\right)\right)\sin\left(\frac{n\pi}{b}\left(y+\frac{b}{2}\right)\right)\right. \\ &\qquad \left. + \underline{y}_o \frac{n\pi}{b}\sin\left(\frac{m\pi}{a}\left(x+\frac{a}{2}\right)\right)\cos\left(\frac{n\pi}{b}\left(y+\frac{b}{2}\right)\right)\right]\end{aligned} \tag{2a}$$

$$\underline{h}'_\upsilon(x,y) = \hat{a}_Z \times \underline{e}'_\upsilon(x,y)$$
$$= A'_\upsilon \left[\underline{x}_o \frac{n\pi}{b} \sin\left(\frac{m\pi}{a}\left(x+\frac{a}{2}\right)\right)\cos\left(\frac{n\pi}{b}\left(y+\frac{b}{2}\right)\right) - \underline{y}_o \frac{m\pi}{a}\cos\left(\frac{m\pi}{a}\left(x+\frac{a}{2}\right)\right)\sin\left(\frac{n\pi}{b}\left(y+\frac{b}{2}\right)\right)\right] \tag{2b}$$

$$\underline{e}''_\upsilon(x,y) = \underline{h}''_\upsilon(x,y) \times \hat{a}_Z$$
$$= A''_\upsilon \left[\underline{x}_o \frac{n\pi}{b} \cos\left(\frac{m\pi}{a}\left(x+\frac{a}{2}\right)\right)\sin\left(\frac{n\pi}{b}\left(y+\frac{b}{2}\right)\right) - \underline{y}_o \frac{m\pi}{a}\sin\left(\frac{m\pi}{a}\left(x+\frac{a}{2}\right)\right)\cos\left(\frac{n\pi}{b}\left(y+\frac{b}{2}\right)\right)\right] \tag{2c}$$

$$\underline{h}''_\upsilon(x,y) = -\nabla_T \Psi_\upsilon(x,y)$$
$$= A''_\upsilon \left[\underline{x}_o \frac{m\pi}{a} \sin\left(\frac{m\pi}{a}\left(x+\frac{a}{2}\right)\right)\cos\left(\frac{n\pi}{b}\left(y+\frac{b}{2}\right)\right) + \underline{y}_o \frac{n\pi}{b}\cos\left(\frac{m\pi}{a}\left(x+\frac{a}{2}\right)\right)\sin\left(\frac{n\pi}{b}\left(y+\frac{b}{2}\right)\right)\right] \tag{2d}$$

where $\Phi_\upsilon(x,y) = A'_\upsilon \sin\left(\frac{m\pi}{a}\left(x+\frac{a}{2}\right)\right)\sin\left(\frac{n\pi}{b}\left(y+\frac{a}{2}\right)\right)$,

$\Psi_\upsilon(x,y) = A''_\upsilon \cos\left(\frac{m\pi}{a}\left(x+\frac{a}{2}\right)\right)\cos\left(\frac{n\pi}{b}\left(y+\frac{b}{2}\right)\right)$, and υ represents the *(m,n)* pair known as the mode number *(5)*. The two mode number indices can take integer values zero or greater. For instance, the TE_{10} mode has mode indices of $m = 1$ and $n = 0$. A'_υ and A''_υ are determined by normalizing equation 2 across the transverse plane of the waveguide in figure 1b as (5)

$$A'^{\,2}_{mn} \int_{-\frac{b}{2}}^{\frac{b}{2}} \int_{-\frac{a}{2}}^{\frac{a}{2}} \underline{e}'_{mn}(x,y) \bullet \underline{e}'_{kl}(x,y)\,dxdy = \delta_{mk}\delta_{nl} \tag{3a}$$

$$A''^{\,2}_{mn} \int_{-\frac{b}{2}}^{\frac{b}{2}} \int_{-\frac{a}{2}}^{\frac{a}{2}} \underline{e}''_{mn}(x,y) \bullet \underline{e}''_{kl}(x,y)\,dxdy = \delta_{mk}\delta_{nl} \tag{3b}$$

where δ is defined as $\delta_{mk} = 0$ for $m \neq k$ and $\delta_{mm} = 0$. Solving equation 3 for the normalization constants yields

$$A'_{mn} = \left(\frac{2}{\pi}\right) \frac{\mathrm{P}_{mn}}{\sqrt{m^2 \frac{a}{b} + n^2 \frac{b}{a}}} \tag{4a}$$

$$A''_{mn} = \left(\frac{\sqrt{\xi_m \xi_n}}{\pi}\right) \frac{\mathrm{P}_{mn}}{\sqrt{m^2 \frac{b}{a} + n^2 \frac{a}{b}}}, \quad \xi_m, \xi_n = \begin{cases} 1; \; m, n = 0 \\ 2; \; m, n = 0 \end{cases} \tag{4b}$$

where P_{mn} is the incident mode's amplitude. Taking equations 2 and 4 into account, we can construct the total transverse E- and H-fields inside the waveguide

$$\begin{aligned} \underline{E}_T(\underline{r}) &= \underline{e}''_N(x,y) e^{-j\kappa_N z} + \vec{\Gamma}''_N(z) \underline{e}''_N(x,y) e^{+j\kappa_N z} \\ &+ \sum_{M \neq N} \left[\vec{\Gamma}'_M(z) \underline{e}'_M(x,y) e^{+j\kappa_M z} + \vec{\Gamma}''_M(z) \underline{e}''_M(x,y) e^{+j\kappa_M z} \right], \quad z \leq 0 \end{aligned} \tag{5a}$$

$$\begin{aligned} \underline{H}_T(\underline{r}) &= Y''_N \underline{h}''_N(x,y) e^{-j\kappa_N z} - Y''_N \vec{\Gamma}''_N(z) \underline{h}''_N(x,y) e^{+j\kappa_N z}) \\ &- \sum_{M \neq N} \left[Y'_M \vec{\Gamma}'_M(z) \underline{h}'_M(x,y) e^{+j\kappa_N z} + Y''_M \Gamma''_M \underline{h}''_M(x,y) e^{+j\kappa_N z} \right], \quad z \leq 0 \end{aligned} \tag{5b}$$

where $\underline{r} = x \cdot \underline{x}_o + y \cdot \underline{y}_o + z \cdot \underline{z}_o$, the subscript M denotes all mode numbers that are not incident on the aperture, and Γ is the reflection coefficient at the aperture. Notice that both the incident and non-incident modes are reflected from the aperture at $z = 0$. Z'_υ, Z''_υ, and κ_υ are defined by

$$Z'_\upsilon = \frac{1}{Y'_\upsilon} = \frac{\kappa_\upsilon}{\omega \varepsilon} \tag{6a}$$

$$Z''_\upsilon = \frac{1}{Y''_\upsilon} = \frac{\omega \mu}{\kappa_\upsilon} \tag{6b}$$

$$\kappa_\upsilon = \sqrt{k^2 - k_{T\upsilon}^2} \tag{6c}$$

$$k_{T\upsilon}^2 = k_x^2 + k_y^2 = \left(\frac{m\pi}{a}\right)^2 + \left(\frac{n\pi}{b}\right)^2 \tag{6d}$$

Here k is the free space wave number and $k_{T\upsilon}$ is the transverse wave number within the waveguide. The equations for the transverse electric and magnetic fields beyond the aperture ($z \geq 0$) can be defined via a Fourier transform as

$$\underline{E}_T(\underline{r}) = \frac{1}{(2\pi)^2} \int_{-\infty}^{\infty} \int_{-\infty}^{\infty} \tilde{\underline{E}}_T(k_x, k_y) e^{-j\underline{k} \bullet \underline{r}} dk_x dk_y, \; z \geq 0 \tag{7a}$$

$$\underline{H}_T(\underline{r}) = \frac{1}{(2\pi)^2} \int_{-\infty}^{\infty} \int_{-\infty}^{\infty} \tilde{\underline{H}}_T(k_x, k_y) e^{-j\underline{k} \bullet \underline{r}} dk_x dk_y, \; z \geq 0 \tag{7b}$$

where the ~ denotes that these components exist in the spectral domain. In order to determine $\underline{\tilde{E}}_T(k_x, k_y)$ and $\underline{\tilde{H}}_T(k_x, k_y)$, we start by equating equations 5 and 7 at z = 0, which is justified by the tangential boundary condition

$$\underline{e}"_N(x,y)(1+\Gamma"_N)+\sum_{M\neq N}\left[\underline{e}'_M(x,y)\Gamma'_M+\underline{e}"_M(x,y)\Gamma"_M\right]=\frac{1}{(2\pi)^2}\int_{-\infty}^{+\infty}\int_{-\infty}^{+\infty}\underline{\tilde{E}}(k_x,k_y)e^{-j\underline{k}_T\bullet\underline{\rho}}dk_xdk_y \quad (8a)$$

$$\begin{aligned}\underline{h}"_N(x,y)Y"_N(1-\Gamma"_N)-\sum_{M\neq N}\Big[Y'_M\,\Gamma'_M\,(z)\,\underline{h}'_M(x,y)\\ +Y"_M\,\Gamma"_M\,\underline{h}"_M(x,y)\Big]=\frac{1}{(2\pi)^2}\int_{-\infty}^{\infty}\int_{-\infty}^{\infty}\underline{\tilde{H}}(k_x,k_y)e^{-j\underline{k}_T\bullet\underline{\rho}}dk_xdk_y\end{aligned} \quad (8b)$$

where $\underline{\rho} = x\cdot\underline{x}_o + y\cdot\underline{y}_o$. Notice that on the right side of equation 8 the $\underline{k} \bullet \underline{r}$ from equation 7 has become $\underline{k} \bullet \underline{\rho}$ at the aperture due to z = 0. The following orthogonality equations (*5*)

$$\int_{-\frac{b}{2}}^{\frac{b}{2}}\int_{-\frac{a}{2}}^{\frac{a}{2}}\underline{e}_k(x,y)\bullet\underline{e}_l(x,y)dxdy=\delta_{kl} \quad (9a)$$

$$\int_{-\frac{b}{2}}^{\frac{b}{2}}\int_{-\frac{a}{2}}^{\frac{a}{2}}\underline{h}_k(x,y)\bullet\underline{h}_l(x,y)dxdy=\delta_{kl} \quad (9b)$$

allow us to simplify equation 8 in terms of the reflection coefficients and spectral components of the E- and H-fields. Here S is the dimensions of the transverse plane of the rectangular waveguide. By limiting the bounds of integration in equation 9, we enforce the boundary condition that $\underline{E}_T(\underline{r})$ = 0 on the surface of the flange. Using the following general substitution

$$\hat{\underline{\alpha}}_\upsilon(\underline{k}_T)=\int_{-\frac{b}{2}}^{\frac{b}{2}}\int_{-\frac{a}{2}}^{\frac{a}{2}}\frac{e^{-j\underline{k}_T\bullet\underline{\rho}}}{(2\pi)^2}\underline{\alpha}_\upsilon(x,y)dxdy \quad (10)$$

we can rewrite equation 8 as the following system of equations:

$$(1+\Gamma"_N)=\int_{-\infty}^{\infty}\int_{-\infty}^{\infty}\left(\hat{\underline{e}}"_N(k_x,k_y)\bullet\underline{\tilde{E}}_T(k_x,k_y)\right)dk_xdk_y=\left(\hat{\underline{e}}"_N(k_x,k_y),\,\underline{\tilde{E}}_T(k_x,k_y)\right) \quad (11a)$$

$$(1-\Gamma"_N)=Z"_N\int_{-\infty}^{\infty}\int_{-\infty}^{\infty}\hat{\underline{h}}"_N(k_x,k_y)\bullet\underline{\tilde{H}}_T(k_x,k_y)dk_xdk_y=Z"_N\left(\hat{\underline{h}}"_N(k_x,k_y),\,\underline{\tilde{H}}_T(k_x,k_y)\right) \quad (11b)$$

$$\Gamma"_M=\left(\hat{\underline{e}}"_M(k_x,k_y),\,\underline{\tilde{E}}_T(k_x,k_y)\right) \quad (11c)$$

$$\Gamma''_M = -Z''_M \left(\underline{\hat{h}}''_N(k_x,k_y),\ \underline{\tilde{H}}_T(k_x,k_y)\right) \tag{11d}$$

$$(1+\Gamma'_N) = \left(\underline{\hat{e}}'_N(k_x,k_y),\ \underline{\tilde{E}}_T(k_x,k_y)\right) \tag{11e}$$

$$(1-\Gamma'_N) = Z'_N \left(\underline{\hat{h}}'_N(k_x,k_y),\ \underline{\tilde{H}}_T(k_x,k_y)\right) \tag{11f}$$

$$\Gamma'_M = \left(\underline{\hat{e}}'_M(k_x,k_y),\ \underline{\tilde{E}}_T(k_x,k_y)\right) \tag{11g}$$

$$\Gamma'_M = -Z''_M \left(\underline{\hat{h}}''_N(k_x,k_y),\ \underline{\tilde{H}}_T(k_x,k_y)\right) \tag{11h}$$

This set of equations are used to solve for $\underline{\tilde{E}}_T(k_x,k_y)$ and $\underline{\tilde{H}}_T(k_x,k_y)$. The solutions to the surface integrals of equation 10 can be determined in closed form and are calculated in the appendix. In order to get equation 11 into matrix form, we need to add like Γ_υ terms together from equation 11. We can now rewrite the entire system of equations using the following two expressions:

$$\left(\underline{\hat{e}}''_\upsilon(k_x,k_y),\ \underline{\tilde{E}}_T(k_x,k_y)\right) + Z''_\upsilon \left(\underline{\hat{h}}''_\upsilon(k_x,k_y),\ \underline{\tilde{H}}_T(k_x,k_y)\right) = 2\delta_{\upsilon N} \tag{12a}$$

$$\left(\underline{\hat{e}}'_\upsilon(k_x,k_y),\ \underline{\tilde{E}}_T(k_x,k_y)\right) + Z'_\upsilon \left(\underline{\hat{h}}'_\upsilon(k_x,k_y),\ \underline{\tilde{H}}_T(k_x,k_y)\right) = 2\delta_{\upsilon N} \tag{12b}$$

3. Formulation of the MDM Method

The basis of the MDM method is the system of equations described by equation 12, which populates the matrix. By representing the integrals in (k_x,k_y) space as a Riemann sum over k_x and k_y, we can formulate the MDM equation.

3.1 Derivation of MDM Equation

To simplify equation 12, we can write equation 7b in terms of equation 7a leaving a single unknown. Starting with the expression (5),

$$\underline{\tilde{H}}_T(k_x,k_y) = \frac{1}{\omega\mu_o}\left[\left(\hat{a}_z \times \underline{\hat{E}}_T(k_x,k_y)\right)k_{z\upsilon} - \left(\frac{\underline{k}_T \times \hat{a}_z}{k_{z\upsilon}}\right)\left(\underline{k}_T \bullet \underline{\hat{E}}_T(k_x,k_y)\right)\right] \tag{13}$$

we can rewrite this as the matrix equation

$$\underline{\tilde{H}}_T(k_x,k_y)=\begin{bmatrix}\widetilde{H}_x(k_x,k_y)\\ \widetilde{H}_y(k_x,k_y)\end{bmatrix}=\begin{bmatrix}A_{xx} & A_{xy}\\ A_{yx} & A_{yy}\end{bmatrix}\begin{bmatrix}\widetilde{E}_x(k_x,k_y)\\ \widetilde{E}_y(k_x,k_y)\end{bmatrix}=\underline{\underline{A}}\bullet\underline{\widehat{E}}_T(k_x,k_y)$$

Evaluating the cross products and dot product of equation 13 yields

$$\begin{aligned}\underline{\tilde{H}}_T(k_x,k_y)&=\frac{1}{\omega\mu_o}\left\{\begin{bmatrix}0 & -\kappa_\upsilon\\ \kappa_\upsilon & 0\end{bmatrix}-\begin{bmatrix}\dfrac{k_xk_y}{\kappa_\upsilon} & \dfrac{k_y^2}{\kappa_\upsilon}\\ -\dfrac{k_x^2}{\kappa_\upsilon} & -\dfrac{k_xk_y}{\kappa_\upsilon}\end{bmatrix}\right\}\begin{bmatrix}\widetilde{E}_x(k_x,k_y)\\ \widetilde{E}_y(k_x,k_y)\end{bmatrix}\\ &=\frac{1}{\omega\mu_o\kappa_\upsilon}\left\{\begin{bmatrix}-k_xk_y & -\left(k_o^2-k_x^2\right)\\ k_o^2-k_y^2 & k_xk_y\end{bmatrix}\right\}\begin{bmatrix}\widetilde{E}_x(k_x,k_y)\\ \widetilde{E}_y(k_x,k_y)\end{bmatrix}=\underline{\underline{A}}\bullet\underline{\widetilde{E}}_T(k_x,k_y)\end{aligned} \tag{14}$$

Equation 12 represents a shorthand notation to represent the system of equations that will construct our MDM equation. However, to properly explain how these equations represent a matrix equation, it is better to think of these equations in longhand notation:

$$\int_{-\infty}^{\infty}\int_{-\infty}^{\infty}\left[\underline{\hat{e}}''_\upsilon(k_x,k_y)+Z''_\upsilon\left(\underline{\underline{A}}\bullet\underline{\hat{h}}''_\upsilon(k_x,k_y)\right)\right]\bullet\underline{\tilde{E}}_T(k_x,k_y)dk_xdk_y=2\delta_{\upsilon N} \tag{15a}$$

$$\int_{-\infty}^{\infty}\int_{-\infty}^{\infty}\left[\underline{\hat{e}}'_\upsilon(k_x,k_y)+Z'_\upsilon\left(\underline{\underline{A}}\bullet\underline{\hat{h}}''_\upsilon(k_x,k_y)\right)\right]\bullet\underline{\tilde{E}}_T(k_x,k_y)dk_xdk_y=2\delta_{\upsilon N} \tag{15b}$$

This set of equations allows us to solve for $\underline{\tilde{E}}_T(k_x,k_y)$. If we redefine the integrals as a Riemann sum, then equation 15 becomes

$$\sum_{k_y}\sum_{k_x}\underbrace{\left[\left(\underline{\hat{e}}''_\upsilon\left(k_x,k_y\right)+Z''_\upsilon\,\underline{\underline{A}}\bullet\underline{\hat{h}}''_\upsilon\left(k_x,k_y\right)\right)\bullet\underline{\tilde{E}}_T\left(k_x,k_y\right)\right]}_{M''_{\upsilon x}\left(k_x,k_y\right)\underline{x}_o+M''_{\upsilon y}\left(k_x,k_y\right)\underline{y}_o}\Delta k_x\Delta k_y=2\delta_{\upsilon N} \tag{16a}$$

$$\sum_{k_y}\sum_{k_x}\underbrace{\left[\left(\underline{\hat{e}}'_\upsilon\left(k_x,k_y\right)+Z'_\upsilon\,\underline{\underline{A}}\bullet\underline{\hat{h}}'_\upsilon\left(k_x,k_y\right)\right)\bullet\underline{\tilde{E}}_T\left(k_x,k_y\right)\right]}_{M'_{\upsilon x}\left(k_x,k_y\right)\underline{x}_o+M'_{\upsilon y}\left(k_x,k_y\right)\underline{y}_o}\Delta k_x\Delta k_y=2\delta_{\upsilon N} \tag{16b}$$

We can now write the MDM equation. In doing so, each value of υ representing a different mode inside the waveguide represents the MDM row index. Since we need an invertible matrix to obtain a solution, υ also represents the discrete index of k_x and k_y in free space, which becomes the column index of our matrix. This creates a square matrix with a total of L samples of k_x and k_y as well as L modes.

$$
2L\left\{\overbrace{\begin{array}{cc}
 & \qquad\qquad \underline{x}_o - direction \qquad\qquad\qquad\qquad\qquad\qquad \underline{y}_o - direction \\
\begin{array}{c} TE \\ \\ \\ \\ \\ TM \end{array} &
\left[\begin{array}{cccc|cccc}
M''_{1x}(\underline{k}_{T1}) & M''_{1x}(\underline{k}_{T2}) & \cdots & M''_{1x}(\underline{k}_{TL}) & M''_{1y}(\underline{k}_{T1}) & M''_{1y}(\underline{k}_{T2}) & \cdots & M''_{1y}(\underline{k}_{TL}) \\
M''_{2x}(\underline{k}_{T1}) & M''_{2x}(\underline{k}_{T2}) & \cdots & M''_{2x}(\underline{k}_{TL}) & M''_{2y}(\underline{k}_{T1}) & M''_{2y}(\underline{k}_{T2}) & \cdots & M''_{2y}(\underline{k}_{TL}) \\
\vdots & \vdots & & \vdots & \vdots & \vdots & & \vdots \\
M''_{Lx}(\underline{k}_{T1}) & M''_{Lx}(\underline{k}_{T2}) & \cdots & M''_{Lx}(\underline{k}_{TL}) & M''_{Ly}(\underline{k}_{T1}) & M''_{Ly}(\underline{k}_{T2}) & \cdots & M''_{Ly}(\underline{k}_{TL}) \\
\hline
M'_{1x}(\underline{k}_{T1}) & M'_{1x}(\underline{k}_{T2}) & \cdots & M'_{1x}(\underline{k}_{TL}) & M'_{1y}(\underline{k}_{T1}) & M'_{1y}(\underline{k}_{T2}) & \cdots & M'_{1y}(\underline{k}_{TL}) \\
M'_{2y}(\underline{k}_{T1}) & M'_{2x}(\underline{k}_{T2}) & \cdots & M'_{2x}(\underline{k}_{TL}) & M'_{2y}(\underline{k}_{T1}) & M'_{2y}(\underline{k}_{T2}) & \cdots & M'_{2y}(\underline{k}_{TL}) \\
\vdots & \vdots & & \vdots & \vdots & \vdots & & \vdots \\
M'_{Nx}(\underline{k}_{T1}) & M'_{Nx}(\underline{k}_{T2}) & \cdots & M'_{Lx}(\underline{k}_{TL}) & M'_{Ly}(\underline{k}_{T1}) & M'_{Ly}(\underline{k}_{T2}) & \cdots & M'_{Ly}(\underline{k}_{TL})
\end{array}\right]
\end{array}}^{2L}\right.
\bullet
\left[\begin{array}{c}
\tilde{E}_x(\underline{k}_{T1}) \\
\tilde{E}_x(\underline{k}_{T2}) \\
\vdots \\
\tilde{E}_x(\underline{k}_{TL}) \\
\hline
\tilde{E}_y(\underline{k}_{T1}) \\
\tilde{E}_y(\underline{k}_{T2}) \\
\vdots \\
\tilde{E}_y(\underline{k}_{TL})
\end{array}\right]
=
\left[\begin{array}{c}
2 \\ 0 \\ \vdots \\ \vdots \\ \vdots \\ \vdots \\ \vdots \\ \vdots \\ \vdots \\ 0
\end{array}\right]
\qquad (17)
$$

In this notation, υ has taken the value of a single integer; however, each row index truly represents a unique wavenumber (m,n) pair. The MDM of equation 17 has four separate quadrants. Quadrant 1 corresponds to the matrix elements that represent the TE modes inside the waveguide in the x-direction, quadrant 2 corresponds to the matrix elements that represent the TE modes inside the waveguide in the y-direction, quadrant 3 corresponds to the matrix elements that represent the TM modes inside the waveguide in the x-direction, and quadrant 4 corresponds to the matrix elements that represent the TM modes inside the waveguide in the y-direction where ($\underline{k}_{T\upsilon}$) is used to represent the (k_x,k_y) pair. The reason the x-components and the y-components of the MDM equation have to be separated is so that the solutions to $\tilde{E}_x(k_x,k_y)$ and $\tilde{E}_y(k_x,k_y)$ can be solved for individually. Each quadrant is L x L in dimension yielding a $2L$ x $2L$ square matrix. The solutions to $\tilde{E}_x(k_x,k_y)$ and $\tilde{E}_y(k_x,k_y)$ are L element vectors. Note that the right-hand side vector of equation 17 is zero except for the first element, which corresponds to the incident TE_{10} mode in the waveguide. This comes directly from the $\delta_{\upsilon N}$ in equation 12.

As with any discrete representation of a continuous function, L must be large enough to ensure an accurate representation of the original function. However, a large L means that many more modes must be used in the MDM equation than are truly necessary to accurately determine the field inside the waveguide. This can lead to a singular matrix, which by definition is not invertible. Therefore, in solving equation 17 we use singular value decomposition (SVD) to determine the pseudo-inverse of the MDM equation. The SVD method is fully described in most linear algebra texts (*6*).

3.2 Representation of $\mathbf{k_x}$ and $\mathbf{k_y}$ When $\mathbf{z \geq 0^+}$

This section describes how to represent the values of k_x and k_y in the MDM equation. Since it is desirable to represent the stationary phase approximation of the far field in spherical coordinates, we must map k_x and k_y to (r,θ,ϕ). The stationary phase approximation is well known and widely used throughout the literature (*5, 7, 8*). The equation is repeated here for convenience:

$$\underline{E}(r,\theta,\phi) \approx j\frac{ke^{-jkr}}{2\pi r}\Big[\underline{\theta}_o\left\{\widetilde{E}_x(k_x,k_y)\cos\phi + \widetilde{E}_y(k_x,k_y)\sin\phi\right\}$$
$$+\,\underline{\phi}_o\left(-\widetilde{E}_x(k_x,k_y)\sin\phi + \widetilde{E}_y(k_x,k_y)\cos\phi\right)\cos\theta\Big] \tag{18}$$

Mapping k_x and k_y to spherical coordinates yields

$$k_x = k_o \sin(\theta)\cos(\phi) \tag{19a}$$

$$k_y = k_o \sin(\theta)\sin(\phi) \tag{19b}$$

In order to get a hemisphere mapping of the radiated far field in the propagation direction, we are interested in values of $-\pi/2 \le \theta \le \pi/2$ and $0 \le \phi \le \pi/2$. After substituting these values of θ and ϕ into equation 19, we get a trajectory of k_x and k_y onto a circle of radius k_o, as shown in figure 2.

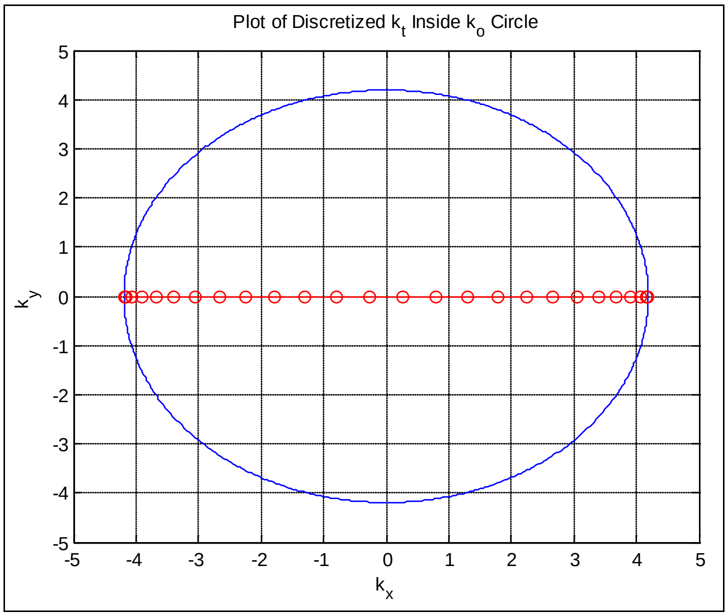

Figure 2. Plot of the values of k_x and k_y obtained for $\phi = 0$.

Figure 2 shows all the k_x and k_y values obtained for $\phi = 0$, $-\pi/2 \le \theta \le \pi/2$, and $\Delta\theta = 1/L$, where L corresponds to the size of each quadrant in the MDM equation. The angle of ϕ is represented in figure 2 as the angle between the k_x and k_y axes. Since $\phi = 0$, all the k_x and k_y values fall on the $k_y = 0$ axis. If we use $\phi = \pi/4$ to calculate k_x and k_y as in figure 3, then we see that the values of k_x and k_y fall on a trajectory that makes an angle of $\pi/4$ with the $k_y = 0$ axis.

Using this technique, we can generate the radiated far field for any value of $0 \le \phi \le \pi/2$. Note that in both figures 2 and 3 an equal spacing between values of θ does not result in an equal spacing in k_x and k_y. Also, any value of k_x and k_y that falls on the k_o radius yields a value of $|\underline{k}_T| = k_o$, which corresponds to $\kappa = 0$. Any value of k_x and k_y that falls beyond the k_o radius corresponds to an imaginary value of κ. These values represent attenuating modes and are not used in the calculations for the incident TE_{10} mode.

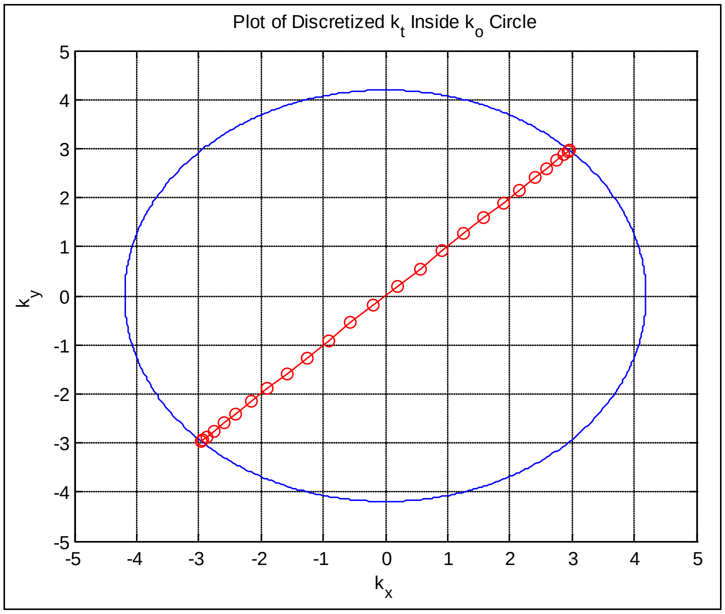

Figure 3. Plot of the values of k_x and k_y obtained for $\phi = \pi/4$.

4. Calculation of Far Field and Comparison to Simulation

This section compares the far-field radiation pattern calculated from the MDM method described in section 3 to those generated using CST Studio Suite 2012. The MDM calculations were performed using Matlab.

4.1 Description of CST Model

Figure 4 depicts the model used to simulate the semi-infinite rectangular waveguide with an infinite flange. Figure 4a gives the transverse dimensions of the waveguide, where $a = \lambda/2$ at 200 MHz and $b = a/2.25$. As long as $a \geq b$, the dominant mode will be the TE_{10} mode. The cutoff frequency for the propagation of the dominant mode is 200 MHz and the cutoff frequency for the next mode to propagate is 400 MHz. For frequencies below 200 MHz, no modes will propagate in the waveguide, and for frequencies above 400 MHz, more than one mode will propagate in the waveguide. Since the method described in section 2 corresponds to a waveguide that is infinite in one direction and ends at a radiating flange at $z = 0$, placing a waveguide port at the end of the waveguide mimics this setup, as shown in figure 4b. The waveguide port will absorb any reflections of additional modes from the aperture to ensure that only the propagating TE_{10} mode will contribute to the far field radiation. The direction of the arrow in figure 4b shows the direction of propagation for the TE_{10} mode.

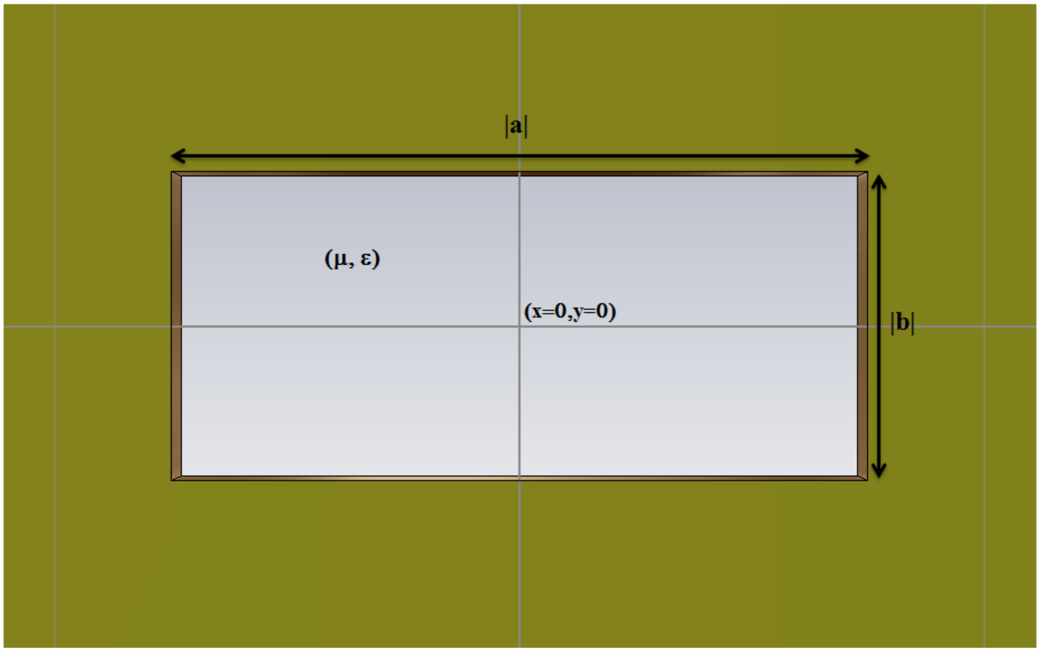

(a)

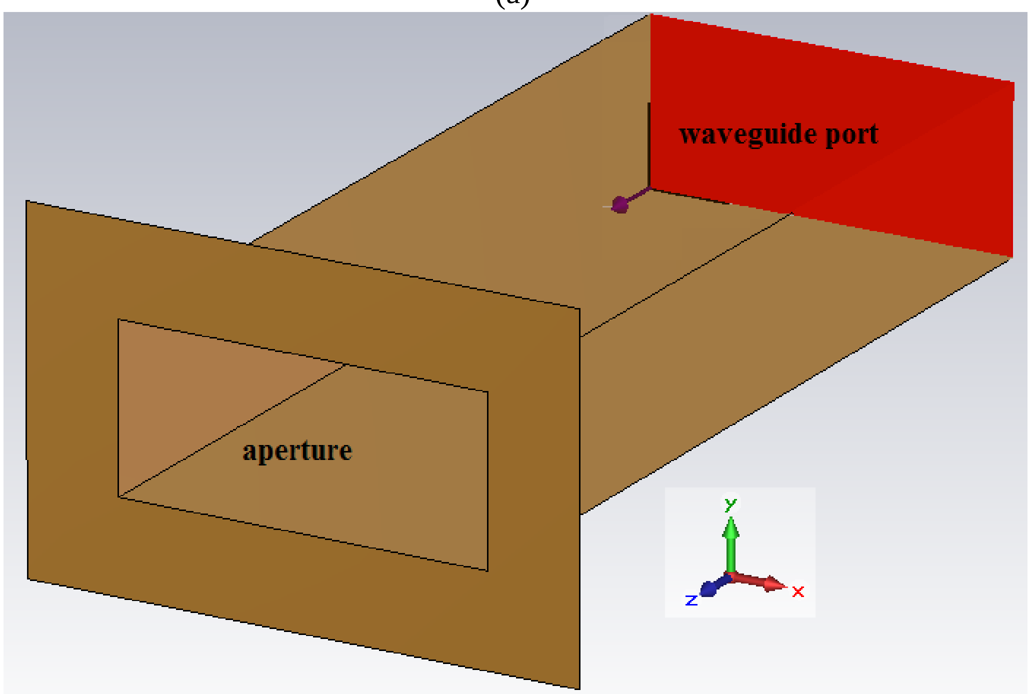

(b)

Figure 4. (a) Transverse plane of the waveguide aperture. The waveguide has dimensions |a| x |b| and is surrounded by an infinite conducting flange. (b) This shows the z-direction of the waveguide with the waveguide port included.

Figure 5 shows the distribution of the mode generated by the waveguide port as a cosine distribution across the long dimension of the waveguide aperture and has units of volts/meter (V/m). This is the expected mode distribution for the TE_{10} mode (*9*). Notice that the mode distribution peaks and is symmetric about x = 0 and y = 0 as expected. The mode distribution does not vary in the z-direction because the mode is propagating and not attenuating.

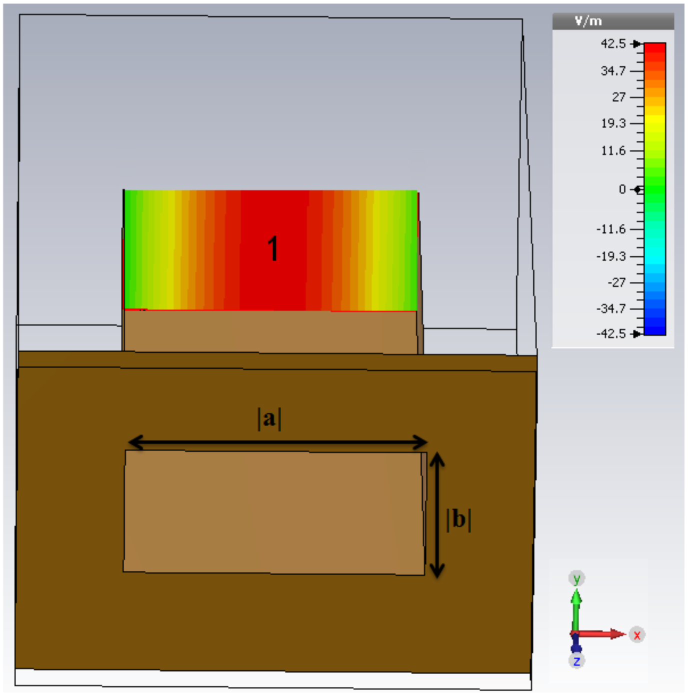

Figure 5. Illustration of the mode distribution in the rectangular waveguide of the infinite flange simulation in V/m.

4.2 Result Analysis

The calculations of the far-field radiation patterns are determined for a frequency of 300 MHz. This frequency was chosen because it stands farthest away from both the cutoff that will not allow the TE_{10} mode to propagate and the cutoff that will allow multiple modes to propagate. The far-field radiation patterns in the $\underline{\theta}_o$ and $\underline{\phi}_o$ directions are calculated from equation 18 as

$$\underline{F}(\theta,\phi) = \underline{\theta}_o \left[\widetilde{E}_x \left(k_x, k_y, z=0\right)\cos\phi + \widetilde{E}_y \left(k_x, k_y, z=0\right)\sin\phi \right] + \underline{\phi}_o \left(-f_x \sin\phi + f_y \cos\phi\right)\cos\theta \qquad (20)$$

Figure 6a shows the patterns of the far field in the F_θ and F_ϕ directions plotted on a polar graph, whereas figure 6b shows the patterns of the far field in the F_θ and F_ϕ directions plotted linearly. These plots assume $\varepsilon_r = 1$ (relative permittivity) and $\mu_r = 1$ (relative permeability) inside the waveguide. We can see from inspection that the results of solving the MDM equation agree very closely with the results generated by the simulation using CST Studio Suite.

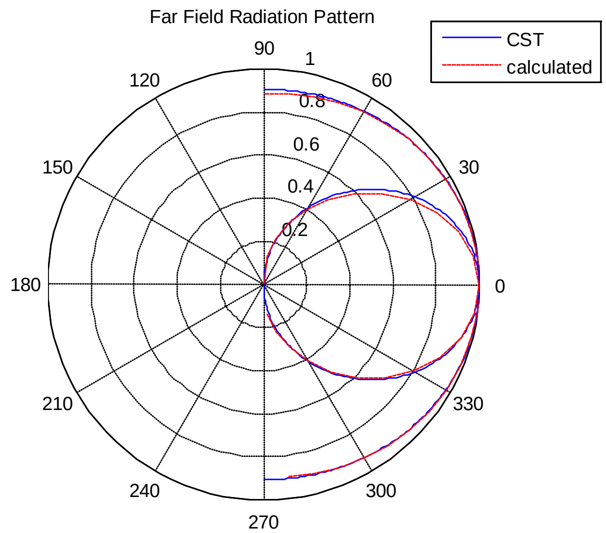

(a)

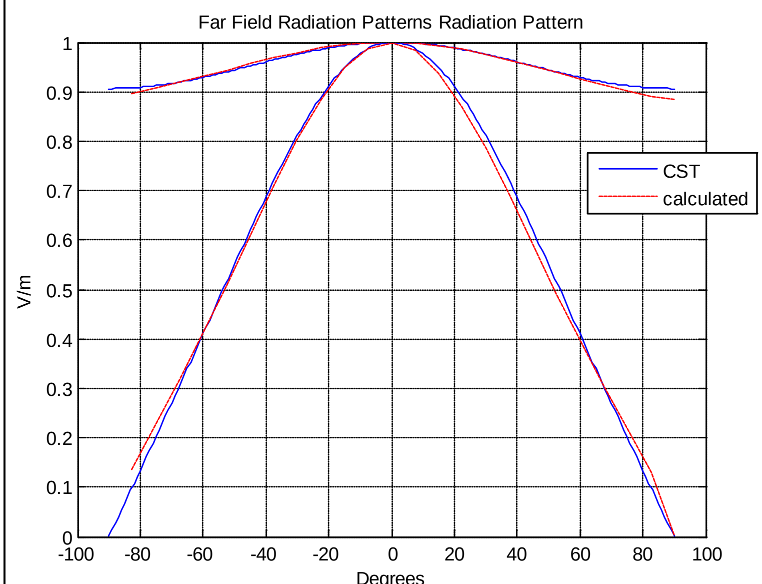

(b)

Figure 6. (a) Polar plot (b) Linear plot - of the far-field F_θ and F_ϕ normalized radiation patterns.

One thing to note is that when using the SVD method in these computations the number of singular values used to generate the pseudo-inverse of the MDM plays a crucial role. A matrix with dimensions 2L x 2L will have 2L singular values. Many of the singular values will have magnitudes approaching zero. These values should not be used or they will affect the accuracy of the numerical results. On the other hand, if one has multiple singular values with useable magnitudes, then eliminating any of them from the calculations will also affect the results. Figure 7 shows a plot of the singular values in descending order for the MDM calculation resulting in the patterns of figure 6. The number of singular values used for this calculation is 4. Generally only the first few singular values are needed.

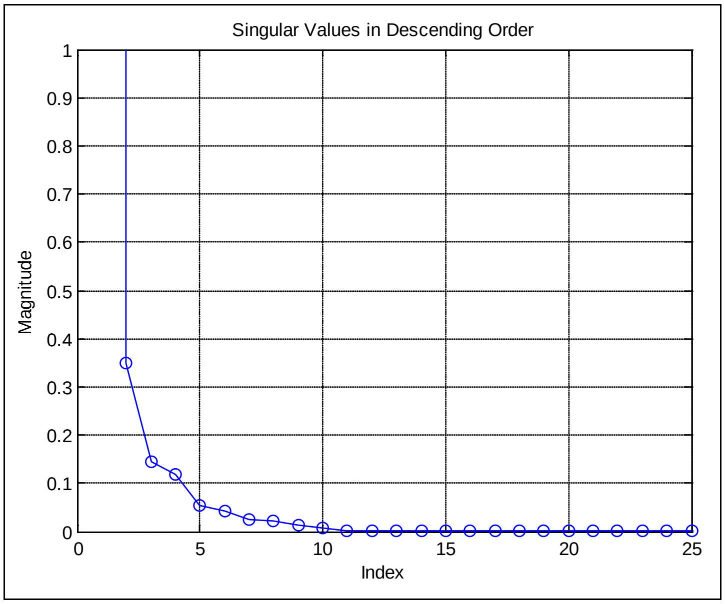

Figure 7. Plot of the singular values of the MDM in descending order.

5. Conclusions

Existing methods for analyzing the radiating infinite flange require the computation of the fields at the aperture. These fields then have to be transformed to the spectral domain before any far-field calculations can be made. This report derives a new approach called the MDM method that allows for the direct computation of the radiated far fields. The result is a matrix equation that directly solves for the spectral components needed for the far-field stationary phase approximation. The results of the MDM method were successfully compared to the far-field radiation patterns of an infinite flange generated by commercial numerical modeling software for the same problem.

6. References

1. MacPhie, R. H.; Zaghloul, A. I. Radiation From a Rectangular Waveguide With Infinite Flange: Exact Solution by Correlation Matrix. *IEEE Trans. Antennas Propagation* **July 1980**, *AP-28*, 497–503.

2. Baudrand, H.; Tao, J.; Atechian, J. Study of Radiation Properties of Open-Ended Rectangular Waveguides. *IEEE Trans. Antennas Propagation* **Aug. 1988**, *36* (8), 1071–1077.

3. Serizawa, H.; Hongo, K. Radiation for a Flanged Rectangular Waveguide. *IEEE Trans. Antennas Propagation* **Dec. 2005**, *53* (12), 3953–3962.

4. Coburn, W.; Anthony, T.; Zahgloul, A. Open-Ended Waveguide Radiation Characteristics – Full-Wave Simulation Versus Analytical Solutions. *Antennas and Propagation Society International Symposium (APSURSI)*, 2010 IEEE.

5. Felsen, L.; Marcuvitz, N. *Radiation and Scattering of Waves*; Englewood Cliffs, NJ: Prentice Hall Inc., 1973.

6. Strang, G. *Introduction to Linear Algebra*; 4th ed.; Wellesley, MA: Cambridge Press, 2009.

7. Balanis, C. *Antenna Theory: Analysis and Design*; 4th ed., Hoboken, NJ: Wiley and Sons Inc., 2005.

8. Ishimaru, A. *Electromagnetic Wave Propagation, Radiation, and Scattering*; Upper Saddle River, NJ: Prentice Hall, 1991.

9. Marcuvitz, N. *Waveguide Handbook*; New York, NY: McGraw-Hill, 1951.

10. Ellis, R. *Calculus with Analytical Geometry*; 5th ed., New York, NY: Thomas Publishing, 1993.

INTENTIONALLY LEFT BLANK.

Appendix. Derivation of Surface Integrals for MDM Equation

This section focuses on the solutions to the surface integrals in equations 10–12. If we assume that the dimensions of our radiating aperture are known and that the dimensions are rectangular with values of $a \geq b$, respectively, then these surface integrals can be solved in closed form. The solutions yield constants, which are used to populate the MDM in equation 17.

A-1 Surface Integrals for TM Modes

We first solve the surface integral that arises from the electric field generated by the TM modes in a rectangular waveguide. The solutions for the incident and non-incident modes have the same form, so we use the symbol υ to denote either N or M.

We start with the following equation, which represents the two dimensional surface integral corresponding to the TM mode vector for the E-field,

$$\hat{\underline{e}}'_{\upsilon}(k_x, k_y) = \int_{-\frac{b}{2}}^{\frac{b}{2}} \int_{-\frac{a}{2}}^{\frac{a}{2}} e^{-j\underline{k}_T \bullet \underline{\rho}} \underline{e}'_{\upsilon}(x, y) dx dy \tag{A-1}$$

where $\underline{e}'_{\upsilon}(x,y)$ is defined by equation 2a. We can extract the x-component and solve for it individually:

$$\hat{e}'_{\upsilon x}(k_x, k_y) = -A'_{\upsilon} \frac{m\pi}{a} \int_{-\frac{a}{2}}^{\frac{a}{2}} \left[e^{-jk_x x} \cos\left(\frac{m\pi}{a}\left(x + \frac{a}{2} \right) \right) dx \right] \int_{-\frac{b}{2}}^{\frac{b}{2}} \left[e^{-jk_y y} \sin\left(\frac{n\pi}{b}\left(y + \frac{b}{2} \right) \right) dy \right] \tag{A-2}$$

If we let

$$I_1(k_y) = \int_{-\frac{b}{2}}^{\frac{b}{2}} \left[e^{-jk_y y} \sin\left(\frac{n\pi}{b}\left(y + \frac{b}{2} \right) \right) dy \right] \tag{A-3a}$$

$$I_2(k_x) = \int_{-\frac{a}{2}}^{\frac{a}{2}} \left[e^{-jk_x x} \cos\left(\frac{m\pi}{a}\left(x + \frac{a}{2} \right) \right) dx \right] \tag{A-3b}$$

then equation A-3a has a known closed-form solution when $k_y \neq 0$ and $n \neq 0$ from (*10*):

$$I_1(k_y) = \frac{e^{-jk_y y}}{-k_y^2 + \left(\frac{q\pi}{b}\right)^2}\left[-jk_y \sin\left(\frac{n\pi}{b}\left(y+\frac{b}{2}\right)\right) - \left(\frac{n\pi}{b}\right)\cos\left(\frac{n\pi}{b}\left(y+\frac{b}{2}\right)\right)\right]\Bigg|_{-\frac{b}{2}}^{\frac{b}{2}}$$

$$= \frac{\left(\frac{n\pi}{b}\right)}{k_y^2 - \left(\frac{n\pi}{b}\right)^2}\left[e^{-jk_y\frac{b}{2}}(-1)^n - e^{+jk_y\frac{b}{2}}\right] \quad k_y \neq 0,\ n = 1,2,3...$$

When $k_y = 0$ and $n \neq 0$, then

$$I_1(k_y) = \int_{-\frac{b}{2}}^{\frac{b}{2}}\left[\sin\left(\frac{n\pi}{b}\left(y+\frac{b}{2}\right)\right)dy\right] = \frac{b}{n\pi}\left(1-(-1)^n\right) \qquad k_y = 0,\ n = 1,2,...$$

Finally, when $n = 0$ then $I_1(ky) = 0$. Similarly, when $k_x \neq 0$ and $m \neq 0$, then

$$I_2(k_x) = \frac{e^{-jk_x x}}{-k_x^2 + \left(\frac{m\pi}{q}\right)^2}\left[-jk_x \cos\left(\frac{m\pi}{a}\left(x+\frac{a}{2}\right)\right) + \frac{m\pi}{a}\sin\left(\frac{m\pi}{a}\left(x+\frac{a}{2}\right)\right)\right]\Bigg|_{-\frac{a}{2}}^{\frac{a}{2}}$$

$$= \frac{jk_x}{k_x^2 - \left(\frac{m\pi}{a}\right)^2}\left[e^{-jk_x\frac{a}{2}}(-1)^m - e^{+jk_x\frac{a}{2}}\right] \quad k_x \neq 0,\ m = 1,2,3...$$

When $k_x = 0$ and $m \neq 0$, then

$$I_2(k_x) = \int_{-\frac{a}{2}}^{\frac{a}{2}}\left[\cos\left(\frac{m\pi}{a}\left(x+\frac{a}{2}\right)\right)dx\right] = 0 \qquad k_x = 0,\ \ m = 1,2,3...$$

and when $m = 0$ and $k_x \neq 0$, then

$$I_2(k_x) = \int_{-\frac{a}{2}}^{\frac{a}{2}} e^{-jk_x x}dx = -jk_x \cos\left(k_x\frac{a}{2}\right) \qquad k_x \neq 0,\ \ m = 0$$

Finally, when $k_x = 0$ and $m = 0$, then

$$I_2(k_x) = \int_{-\frac{a}{2}}^{\frac{a}{2}} dx = a \quad k_x = 0,\ m = 0$$

Therefore, the final form of equation A-3 is

$$I_1(k_y) = \begin{cases} \dfrac{\left(\dfrac{n\pi}{b}\right)}{k_y^2 - \left(\dfrac{n\pi}{b}\right)^2}\left[e^{-jk_y\frac{b}{2}}(-1)^n - e^{+jk_y\frac{b}{2}}\right], & k_y \neq 0,\ n = 1,2,3... \\ 0, & n = 0 \\ \dfrac{b}{n\pi}\left(1-(-1)^n\right), & k_y = 0,\ n = 1,2,3.. \end{cases} \tag{A-4a}$$

$$I_2(k_x) = \begin{cases} \dfrac{jk_x}{k_x^2 - \left(\dfrac{m\pi}{a}\right)^2}\left[e^{-jk_x\frac{a}{2}}(-1)^m - e^{+jk_x\frac{a}{2}}\right], & k_x \neq 0,\ m = 1,2,3... \\ 0, & k_x = 0,\ m = 1,2,3... \\ -jk_x \cos\left(k_x \dfrac{a}{2}\right), & k_x \neq 0,\ m = 0 \\ a, & k_x = 0,\ m = 0 \end{cases} \tag{A-4b}$$

Now that we have closed-form solutions for the integrals I_1 and I_2, we can determine the final form of A-2 as

$$\hat{e}'_{\upsilon x}(k_x, k_y) = -A'_\upsilon \frac{m\pi}{a} I_1(k_y) I_2(k_x) \tag{A-5}$$

Similarly, we can extract the y-component from equation A-1 and solve for it individually as

$$\hat{e}'_{\upsilon y}(k_x, k_y) = -A'_\upsilon \frac{n\pi}{b} \int_{-\frac{a}{2}}^{\frac{a}{2}} \left[e^{-jk_x x} \sin\left(\frac{m\pi}{a}\left(x + \frac{a}{2}\right)\right) dx\right] \int_{-\frac{b}{2}}^{\frac{b}{2}} \left[e^{-jk_y y} \cos\left(\frac{n\pi}{b}\left(y + \frac{b}{2}\right)\right) dy\right] \tag{A-6}$$

If we let

$$I_3(k_y) = \int_{-\frac{b}{2}}^{\frac{b}{2}} \left[e^{-jk_y y} \cos\left(\frac{n\pi}{b}\left(y + \frac{b}{2}\right)\right) dy\right] \tag{A-7a}$$

$$I_4(k_x) = \int_{-\frac{a}{2}}^{\frac{a}{2}} \left[e^{-jk_x x} \sin\left(\frac{m\pi}{a}\left(x + \frac{a}{2} \right) \right) dx \right] \tag{A-7b}$$

then using the same analysis we used to solve the integrals of equation A-3 we can write equation A-7 as

$$I_3(k_y) = \begin{cases} \dfrac{jk_y}{k_y^2 - \left(\dfrac{n\pi}{b}\right)^2} \left[e^{-jk_y \frac{b}{2}} (-1)^n - e^{+jk_y \frac{b}{2}} \right], & k_y \neq 0,\ n = 1, 2, 3... \\ 0, & k_y = 0,\ n = 1, 2, 3... \\ -jk_y \cos\left(k_y \dfrac{b}{2} \right), & k_y \neq 0,\ n = 0 \\ b, & k_y = 0,\ n = 0 \end{cases} \tag{A-8a}$$

$$I_4(k_x) = \begin{cases} \dfrac{\left(\dfrac{m\pi}{a}\right)}{k_x^2 - \left(\dfrac{m\pi}{a}\right)^2} \left[e^{-jk_x \frac{a}{2}} (-1)^m - e^{+jk_x \frac{a}{2}} \right], & k_x \neq 0,\ m = 1, 2, 3... \\ 0, & m = 0 \\ \dfrac{a}{m\pi}\left(1 - (-1)^m\right), & k_x = 0,\ m = 1, 2, 3,.. \end{cases} \tag{A-8b}$$

Now that we have closed-form solutions for the integrals I_3 and I_4, we can determine the final form of A-6 as

$$\hat{e}'_{\upsilon y}(k_x, k_y) = -A'_\upsilon \frac{n\pi}{b} I_3(k_y) I_4(k_x) \tag{A-9}$$

Now we solve the surface integral that arises from the magnetic field generated by the TM modes in a rectangular waveguide. We begin with the following equation, which represents the two-dimensional surface integral corresponding to the TM mode vector for the H-field,

$$\underline{\hat{h}}'_\upsilon(k_x, k_y) = \int_{-\frac{b}{2}}^{\frac{b}{2}} \int_{-\frac{a}{2}}^{\frac{a}{2}} e^{-j\underline{k}_T \bullet \underline{\rho}}\, \underline{h}'_\upsilon(x, y) dx dy \tag{A-10}$$

where $\underline{h}'_\upsilon(x,y)$ is defined by equation 2b. We can extract the x-component and solve for it individually:

$$\hat{h}'_{\upsilon x}(k_x,k_y) = A'_\upsilon \frac{n\pi}{b} \int_{-\frac{a}{2}}^{\frac{a}{2}} \left[e^{-jk_x x} \sin\left(\frac{m\pi}{a}\left(x+\frac{a}{2}\right)\right) dx \right] \int_{-\frac{b}{2}}^{\frac{b}{2}} \left[e^{-jk_y y} \cos\left(\frac{n\pi}{b}\left(y+\frac{b}{2}\right)\right) dy \right] \tag{A-11}$$

We see that these are the same integrals as those of equation A-6, and we can write the solution to A-11 as

$$\hat{h}'_{\upsilon x}(k_x,k_y) = A'_\upsilon \frac{n\pi}{b} I_3(k_y) I_4(k_x) \tag{A-12}$$

Similarly, we can extract the y-component from equation 2b and solve for it individually:

$$\hat{h}'_{\upsilon y}(k_x,k_y) = -A'_\upsilon \frac{m\pi}{a} \int_{-\frac{a}{2}}^{\frac{a}{2}} \left[e^{-jk_x x} \cos\left(\frac{m\pi}{a}\left(x+\frac{a}{2}\right)\right) dx \right] \int_{-\frac{b}{2}}^{\frac{b}{2}} \left[e^{-jk_y y} \sin\left(\frac{n\pi}{b}\left(y+\frac{b}{2}\right)\right) dy \right] \tag{A-13}$$

We see that these are the same integrals as those of equation A-2, and we can write the solution to A-13 as

$$\hat{h}'_{\upsilon y}(k_x,k_y) = -A'_\upsilon \frac{m\pi}{a} I_1(k_y) I_2(k_x) \tag{A-14}$$

We can now rewrite equation 12b in terms of equations A-5, A-9, A-12, and A-14 as

$$\begin{aligned} &\left(\left[\hat{e}'_{\upsilon x}(k_x,k_y)\underline{x}_o + \hat{e}'_{\upsilon y}(k_x,k_y)\underline{y}_o \right], \underline{\tilde{E}}_T(k_x,k_y) \right) \\ &\qquad + Z'_\upsilon \left(\underline{\underline{A}} \bullet \left[\hat{h}'_{\upsilon x}(k_x,k_y)\underline{x}_o + \hat{h}'_{\upsilon y}(k_x,k_y)\underline{y}_o \right], \underline{\tilde{E}}_T(k_x,k_y) \right) = 2\delta_{\upsilon N} \end{aligned} \tag{A-15}$$

Equation A-15 represents the final form that we need to determine our system of equations for the TM modes.

A-2 Surface Integrals for TE Modes

Now we solve the surface integral arising from the electric field generated by the TE modes in the rectangular waveguide. We begin with the following equation, which represents the two-dimensional surface integral corresponding to the TE mode vector for the E-field,

$$\hat{\underline{e}}''_\upsilon(k_x,k_y) = \int_{-\frac{b}{2}}^{\frac{b}{2}} \int_{-\frac{a}{2}}^{\frac{a}{2}} e^{-j\underline{k}_T \bullet \underline{\rho}} \underline{e}''_\upsilon(x,y)\,dxdy \tag{A-16}$$

where $\underline{e}''_\upsilon(k_x,k_y)$ is defined by equation 2c. We can extract the x-component and solve for it individually:

$$\hat{e}''_{\upsilon x}(k_x,k_y) = A''_{\upsilon}\frac{n\pi}{b}\int_{-\frac{a}{2}}^{\frac{a}{2}} e^{-jk_x x}\cos\left(\frac{m\pi}{a}\left(x+\frac{a}{2}\right)\right)dx\int_{-\frac{b}{2}}^{\frac{b}{2}} e^{-jk_y y}\sin\left(\frac{n\pi}{b}\left(y+\frac{b}{2}\right)\right)dy \tag{A-17}$$

We see that these are the same integrals as those of equation A-2 and we can write the solution to A-17 as

$$\hat{e}''_{\upsilon x}(k_x,k_y) = \frac{2n\pi}{b\sqrt{ab}} I_1(k_y)I_2(k_x) \tag{A-18}$$

Similarly, we can extract the y-component from equation 2c and solve for it individually:

$$\hat{e}''_{\upsilon y}(k_x,k_y) = -A''_{\upsilon}\frac{m\pi}{a}\int_{-\frac{a}{2}}^{\frac{a}{2}} e^{-jk_x x}\sin\left(\frac{m\pi}{a}\left(x+\frac{a}{2}\right)\right)dx\int_{-\frac{b}{2}}^{\frac{b}{2}} e^{-jk_y y}\cos\left(\frac{n\pi}{b}\left(y+\frac{b}{2}\right)\right)dy \tag{A-19}$$

We see that these are the same integrals as those of equation A-6 and we can write the solution to A-19 as

$$\hat{e}''_{\upsilon y}(k_x,k_y) = -\frac{2m\pi}{a\sqrt{ab}} I_3(k_y)I_4(k_x) \tag{A-20}$$

Now we can solve the surface integral arising from the magnetic field generated by the TE modes in the rectangular waveguide. Beginning with the following equation, which represents the two dimensional surface integral corresponding to the TE mode vector for the H-field,

$$\underline{\hat{h}}''_{\upsilon}(k_x,k_y) = \int_{-\frac{b}{2}}^{\frac{b}{2}}\int_{-\frac{a}{2}}^{\frac{a}{2}} e^{-j\underline{k}_T\bullet\underline{\rho}}\,\underline{h}''_{\upsilon}(x,y)dxdy \tag{A-21}$$

where $\underline{h}''_{\upsilon}(k_x,k_y)$ is defined by equation 2d. We can extract the x-component and solve for it individually:

$$\hat{h}''_{\upsilon x}(k_x,k_y) = A''_{\upsilon}\frac{m\pi}{a}\int_{-\frac{a}{2}}^{\frac{a}{2}}\left[e^{-jk_x x}\sin\left(\frac{m\pi}{a}\left(x+\frac{a}{2}\right)\right)dx\right]\int_{-\frac{b}{2}}^{\frac{b}{2}}\left[e^{-jk_y y}\cos\left(\frac{n\pi}{b}\left(y+\frac{b}{2}\right)\right)dy\right] \tag{A-22}$$

We see that these are the same integrals as those of equation A-6, and we can write the solution to A-22 as

$$\hat{h}''_{\upsilon x}(k_x,k_y) = A''_{\upsilon}\frac{m\pi}{a} I_3(k_y)I_4(k_x) \tag{A-23}$$

Similarly, we can extract the y-component from equation 2d and solve for it individually:

$$\hat{h}''_{\upsilon y}(k_x,k_y) = A'_\upsilon \frac{n\pi}{b} \int_{-\frac{a}{2}}^{\frac{a}{2}} \left[e^{-jk_x x} \cos\left(\frac{m\pi}{a}\left(x+\frac{a}{2}\right)\right) dx \right] \int_{-\frac{b}{2}}^{\frac{b}{2}} \left[e^{-jk_y y} \sin\left(\frac{n\pi}{b}\left(y+\frac{b}{2}\right)\right) dy \right] \tag{A-24}$$

We see that these are the same integrals as those of equation A-2, and we can write the solution to A-24 as

$$\hat{h}''_{\upsilon y}(k_x,k_y) = A''_\upsilon \frac{n\pi}{b} I_1(k_y) I_2(k_x) \tag{A-25}$$

We can now rewrite equation 12a in terms of equations A-18, A-20, A-23, and A-25 as

$$\begin{aligned} &\left(\left[\hat{e}''_{\upsilon x}(k_x,k_y)\underline{x}_o + \hat{e}''_{\upsilon y}(k_x,k_y)\underline{y}_o\right], \underline{\tilde{E}}_T(\underline{k}_T)\right) \\ &\quad + Z''_\upsilon\left(\underline{\underline{A}}\bullet\left[\hat{h}''_{\upsilon x}(k_x,k_y)\underline{x}_o + \hat{h}''_{\upsilon y}(k_x,k_y)\underline{y}_o\right], \underline{\tilde{E}}_T(\underline{k}_T)\right) = 2\delta_{\upsilon N} \end{aligned} \tag{A-26}$$

Equation A-26 represents the final form that we need to determine our system of equations for the TE modes.

List of Symbols, Abbreviations, and Acronyms

FDTD	finite-difference time-domain
MDM	modal decomposition matrix
MHz	megahertz
SVD	singular value decomposition
TE_{10}	transverse electric with mode number *(1,0)*
TM	transverse magnetic
V/m	volts/meter

NO. OF COPIES	ORGANIZATION
1 (PDF)	DEFENSE TECHNICAL INFORMATION CTR DTIC OCA
2 (PDFS)	DIRECTOR US ARMY RESEARCH LAB RDRL CIO LL IMAL HRA MAIL & RECORDS MGMT
1 (PDF)	GOVT PRINTG OFC A MALHOTRA
3 (PDFS)	DIRECTOR RDRL SER M E ADLER G MITCHELL S WEISS

INTENTIONALLY LEFT BLANK.